Acta Crystallographica Section D
Biological Crystallography
ISSN 0907-4449

The structure of plastocyanin from the cyanobacterium *Phormidium laminosum*

Charles S. Bond,[a] Derek S. Bendall,[b] Hans C. Freeman,[c]* J. Mitchell Guss,[a] Christopher J. Howe,[b] Michael J. Wagner[b] and Matthew C. J. Wilce[a]

[a]Department of Biochemistry, University of Sydney, NSW 2006, Australia, [b]Cambridge Centre for Molecular Recognition and Department of Biochemistry, University of Cambridge, Tennis Court Road, Cambridge CB2 1QW, England, and [c]School of Chemistry, University of Sydney, NSW 2006, Australia

Correspondence e-mail: freemanh@chem.usyd.edu.au

Received 8 June 1998
Accepted 21 September 1998

PDB Reference: plastocyanin, 1baw.

The crystal structure of the 'blue' copper protein plastocyanin from the cyanobacterium *Phormidium laminosum* has been solved and refined using 2.8 Å X-ray data. *P. laminosum* plastocyanin crystallizes in space group $P4_32_12$ with unit-cell dimensions a = 86.57, c = 91.47 Å and with three protein molecules per asymmetric unit. The final residual R is 19.9%. The structure was solved using molecular replacement with a search model based on the crystal structure of a close homologue, *Anabaena variabilis* plastocyanin (66% sequence identity). The molecule of *P. laminosum* plastocyanin has 105 amino-acid residues. The single Cu atom is coordinated by the same residues – two histidines, a cysteine and a methionine – as in other plastocyanins. In the crystal structure, the three molecules of the asymmetric unit are related by a non-crystallographic threefold axis. A Zn atom lies between each pair of neighbouring molecules in this ensemble, being coordinated by a surface histidine residue of one molecule and by two aspartates of the other.

1. Introduction

Plastocyanin is a small (M_r 10000–12000) 'blue' copper protein ('type 1', 'cupredoxin'). It plays an essential role in oxygenic photosynthesis, where its function is to carry electrons from the cytochrome b_6f complex to the $P700^+$ complex of Photosystem I (PSI). Its reactions with cytochrome f and $P700^+$ are interesting examples of long-range electron transfer in proteins. These reactions have been intensively studied for the proteins and complexes of higher plants, but a full understanding in terms of the molecular structures and physical properties of the proteins concerned remains elusive (Redinbo *et al.*, 1994). All known higher plant plastocyanins have a negative overall charge, and it is clear that the diffusive interactions of plastocyanin with its reaction partners are strongly influenced by the electrostatic properties of the molecules. A group of conserved acidic residues at the so-called 'remote' site has been implicated (Lee *et al.*, 1995; Kannt *et al.*, 1996; Hibino *et al.*, 1996; Hippler *et al.*, 1996). Recent NMR evidence favours a two-step mechanism in which the acidic residues on plastocyanin initially provide electrostatic guidance for 'docking' with a group of basic residues on cytochrome f (Ubbink *et al.*, 1998). The transient bimolecular complex formed in this way is thought to have many rapidly exchanging orientations and to undergo a rearrangement which establishes an electron-transfer pathway by bringing His87 (the 'northern' histidine) of plastocyanin into contact with the haem group of the cytochrome (Ubbink *et al.*, 1998). Plastocyanins from cyanobacteria, on the other hand, have only a small negative or even a positive total charge, and

Table 1
Data-processing and merging statistics.

77 432 observations, overall completeness of 99.9%.

Resolution range (Å)	Number of unique reflections	Mean $I/\sigma(I)$	R_{merge}†
50.00–6.02	998	25.8	0.058
6.02–4.78	926	23.1	0.074
4.78–4.18	914	23.5	0.081
4.18–3.80	898	18.9	0.099
3.80–3.53	907	16.4	0.113
3.53–3.32	866	10.5	0.155
3.32–3.15	888	8.5	0.197
3.15–3.02	892	7.0	0.223
3.02–2.90	877	5.7	0.271
2.90–2.80	815	4.1	0.359
50.00–2.80	8981	15.1	0.114

† $R_{merge} = \sum|I - \langle I\rangle| / \sum\langle I\rangle$.

sequence alignments indicate that the conserved acidic residues of the plant proteins have largely been replaced by neutral or basic residues. The finding that electron transfer to the plastocyanin of the cyanobacterium *Synechocystis* sp. PCC6803 occurs *via* a collisional mechanism has been attributed to the absence of an acidic patch (Romero *et al.*, 1998). In the case of the weakly acidic (p*I* 5.2) plastocyanin from the cyanobacterium *Phormidium laminosum*, the effects of ionic strength on the reaction with the cytochrome b_6f complex suggest that the electrostatic interactions found in plants are reversed, and that local positive charges on plastocyanin attract local negative charges on cytochrome *f* (Wagner *et al.*, 1996). The need to explain this interaction in molecular terms led to an interest in the molecular structure and thus provided the motivation for the present work.

2. Materials and methods

2.1. Protein expression and purification

The starting point for the preparation of recombinant plastocyanin of *P. laminosum* (PlPc) was the plasmid pPLL6B, which included a DNA fragment containing the *petE* gene and flanking regions (Varley *et al.*, 1995). The sequence corresponding to the mature protein plus its leader sequence was amplified by the polymerase chain reaction and used to prepare a plasmid (pETPC) derived from the high expression plasmid pET11d. The construct was used to transform *E. coli* BL21(DE3)pLysS. The transformed cells were grown overnight on plates containing ampicillin. Recombinants were isolated and used for preparation of plastocyanin.

PlPc was expressed in *E. coli* BL21(DE3)pLysS grown overnight in the presence of 100 µ*M* copper acetate, 0.2 m*M* isopropylthio-β-D-galactoside as inducer and 100 µg ml^{-1} ampicillin. Mature protein was secreted into the periplasmic space. After harvesting the cells, the periplasmic contents were obtained by osmotic shock and the protein was purified by a series of chromatographic procedures involving ion exchange and gel filtration with the protein in both oxidized and reduced states. The absorbance ratio A_{278}/A_{598} for the pure oxidized protein was 2.0.

The recombinant protein was shown to be identical with a sample of native plastocyanin isolated directly from cells of *P. laminosum* (Varley *et al.*, 1995) by UV/visible spectroscopy, one-dimensional ^{1}H NMR spectrometry, electrospray mass spectrometry, redox potentiometry and isoelectric focusing. Full details of the above methods and results will be provided elsewhere.

In order to ensure that the protein used for crystallization had metal sites fully occupied by Cu^{II}, 1 ml of PlPc solution was concentrated from 1.36 to 9 mg ml^{-1} in a Centricon (Millipore; cutoff 1 kDa) with successive washes of 2 ml of 1 m*M* $CuCl_2$, 3 ml of 0.1 *M* Tris (pH 8), 2 ml of 1 m*M* potassium ferricyanide and 3 ml of Tris.

2.2. Crystallization, data collection and processing

PlPc was initially crystallized from Hampton Crystal Screen 1 condition #45 (Hampton Research Ltd). A fine search around this condition gave the best crystals in 0.1 *M* sodium cacodylate buffer pH 6.0, 0.2 *M* zinc acetate and 15%(*v*/*v*) PEG 8000. The square-pyramidal blue crystals grew to 0.35 × 0.28 × 0.28 mm in several weeks at 277 K. No crystals were obtained in the absence of zinc acetate.

X-ray data were recorded on an R-AXIS II imaging-plate detector mounted on an RU-200 rotating-anode generator with a Cu target and focusing-mirror optics (Z. Otwinowski & G. Johnson, Yale University, as marketed by Molecular Structure Corporation, Texas, USA). All data were integrated and scaled with *DENZO* and *SCALEPACK* (Otwinowski, 1993). Native data to 2.8 Å were collected at 293 K from three crystals ($P4_32_12$; $a = 86.57$, $c = 91.47$ Å, $Z = 24$, three molecules per asymmetric unit). Details of data-merging statistics are given in Table 1.

2.3. Structure analysis and refinement

The structure was solved by molecular replacement (MR) using *AMoRe* (Collaborative Computational Project, Number 4, 1994; Navaza, 1994). The search model was taken from the crystal structure of *Anabaena variabilis* plastocyanin (AvPc) at 1.7 Å resolution (Fields *et al.*, 1999). The amino-acid sequence of PlPc is 66% identical to that of AvPc, with no insertions, deletions or terminal extensions. The search model comprised one of the two nearly identical molecules in the asymmetric unit of AvPc, with non-glycine residues truncated at Cβ. The active-site Cu atom was omitted in order to provide a means of validating subsequent MR solutions.

A self-rotation function was calculated, but was not interpretable since the number of molecules in the asymmetric unit was not known unequivocally. The calculated values of the solvent content V_M for two or four molecules per asymmetric unit, 3.7 or 1.9 Å^3 Da^{-1}, were both within the range normally observed (Matthews, 1977). When the structure was eventually solved, it was found to be consistent with the self-rotation function (see below). A cross-rotation function (RF) was calculated using normalized structure-factor amplitudes

Table 2
Refinement statistics.

Resolution range (Å)	Number of reflections		Residual R	
	Working	Test	Working	Test
50.00–5.60	1146	53	0.1985	0.2637
5.60–4.44	1100	51	0.1543	0.1564
4.44–3.88	1069	51	0.1583	0.2096
3.88–3.53	1055	62	0.1886	0.2755
3.53–3.27	1046	60	0.2248	0.2756
3.27–3.08	1062	43	0.2401	0.2956
3.08–2.93	1038	48	0.2569	0.3321
2.93–2.80	1037	60	0.2728	0.3586
50.00–2.80	8553	428	0.1985	0.2524

Table 3
Average temperature factors for groups of atoms in *P. laminosum* plastocyanin.

Group	Number of atoms	Average temperature factor (Å^2)
All atoms	2460	34
Molecule A	805	31
Molecule B	805	25
Molecule C	805	39
Cu	3	28
Zn	3	30
Cu ligands†	12	22
Solvent	39	48

† His39 $N^{\delta1}$, Cys89 S^{γ}, His92 $N^{\delta1}$, Met97 S^{δ}.

(Driessen & Tickle, 1994) in the resolution range 10–3 Å using *AMoRe*. The top 100 solutions from the RF progressed to the translation function (TF) stage. TF and fit-function (FF) calculations were carried out in the enantiomorphic space groups $P4_12_12$ and $P4_32_12$. The solutions in space group $P4_32_12$ had a higher self-consistency and statistical significance.

The positions of the three molecules comprising the final solution were found in a stepwise manner. In space group $P4_32_12$, the best FF solution [$(\theta_1, \theta_2, \theta_3) = (33.0, 42.6, 320.7^\circ)$, $(x, y, z) = (0.337, 0.390, 0.261)$; 4.5σ] was fixed, and was used to phase a further round of TF/FF. This yielded a second significant peak [$(\theta_1, \theta_2, \theta_3) = (64.9, 55.4, 184.14^\circ)$, $(x, y, z) = (0.146, 0.116, 0.701)$]. A third round of TF/FF, in which both solutions were fixed, yielded a third peak [$(\theta_1, \theta_2, \theta_3) = (32.8, 66.3, 78.6^\circ)$, $(x, y, z) = (0.886, 0.593, 0.548)$]. The molecules corresponding to these three solutions were found to be related by a non-crystallographic threefold rotation axis, which was consistent with the peak at $\omega = 54.7$, $\varphi = 45.0$, $\kappa = 120^\circ$ in the self-rotation function calculated with *POLARRFN* (Collaborative Computational Project, Number 4, 1994). An ($\big||F_o| - |F_c|\big|$, α_{calc}) electron-density difference map calculated from these coordinates contained a strong well defined peak at the putative Cu-atom position of each of the three molecules. Rigid-body refinement in *X-PLOR* (Brünger, 1992), in which first the trimer and then the three separate molecules were treated as rigid bodies, led to small decreases in the residuals R (from 48.1 to 47.9%) and R_{free} (from 49.4 to 48.3%). The value of R_{free} in these and subsequent refinement calculations was calculated using a subset of 428 randomly selected reflections (5% of the total), which were otherwise excluded from the refinement. At this point, non-crystallographic symmetry (NCS) matrices were derived from the three monomers, and threefold cyclic map averaging was performed with the *RAVE* package (Kleywegt & Jones, 1994*a*). The resulting averaged map was of good quality, permitting the addition of all side chains to the poly-Gly/Ala model. Map inspection and rebuilding were performed using *O* (Jones *et al.*, 1991).

Refinement in *X-PLOR* continued with simulated annealing. Strict NCS constraints and a bulk-solvent correction were applied, yielding residuals $R = 36.2\%$ and $R_{free} = 40.6\%$. The Cu atom was added to the single-molecule model. Further refinement of the positional and temperature parameters, using two isotropic B values per residue, reduced the residuals to $R = 27.1\%$ and $R_{free} = 27.9\%$. A new threefold-averaged map was calculated and the model was rebuilt to fit this map.

The strict NCS contraints were now replaced by restraints [main-chain atoms: weight = 300, $\sigma(B) = 1$; side-chain atoms: weight = 200, $\sigma(B) = 2$]. As the refinement progressed, electron-density maps revealed significant deviations from NCS at residues 1, 10–12, 24–28, 54, 77–81 and 104–105. The restraints at these residues were relaxed further [weight = 5, $\sigma(B) = 5$]. The refinement of positional and temperature parameters as above converged with residuals $R = 21.1\%$ and $R_{free} = 26.2\%$.

In the final rounds of refinement, cycles of rebuilding and omit-map calculation allowed the less well defined regions of electron density to be modelled confidently and with minimal model bias. Solvent molecules were added at 39 difference-density peaks exceeding $3\sigma(\rho)$, each peak having at least one hydrogen-bonding partner at a geometrically appropriate position. In order to minimize model bias in the Cu–ligand distances, the van der Waals interaction restraints were removed from the ligand residues (His39, Cys89, His92 and Met97) and the Cu atom. A notable feature of the final refinement cycles was the persistence of three large NCS-related difference-density peaks, one between each pair of molecules in the trimer. Test refinements of the B values, in which the peaks were modelled as solvent or metal atoms of various sizes, suggested the presence of metal atoms with about 30 electrons. The peaks could be assigned with high probability as Zn^{2+} ions, on the grounds that the crystallization buffer had contained 0.2 M Zn^{2+}. The tetrahedral arrangement of the nearest neighbours, which include the side chains of a histidine in one protein molecule and two aspartates in another, supported the assignment.

The final model consists of 2418 protein atoms, three Cu atoms, three Zn atoms and 39 ordered solvent molecules; the atomic coordinates were deposited with the Protein Data Bank (Bernstein *et al.*, 1977). The final values of the residuals are $R = 19.9\%$ and $R_{free} = 25.2\%$ (Table 2). The r.m.s. deviations of the geometry from the Engh & Huber (1991) dictionary are: bonds, 0.009 Å; angles, 1.8°; dihedrals, 27.3° and impropers (Cα tetrahedral distortion values), 1.8°. In a Ramachandran plot (not shown) calculated with *MOLEMAN* (Kleywegt & Jones, 1996), only one non-glycine residue is in

the less favoured region. The average displacement parameters for various groups of atoms are given in Table 3.

The value of $\sigma_w(x)$, the 'diffraction data precision indicator' (Cruickshank, 1996) for an average atom is 0.7 Å. Corresponding values for poplar plastocyanin (PoPc) at 1.3 Å resolution and AvPc at 1.7 Å resolution are 0.06 and 0.11 Å, respectively. The higher $\sigma_w(x)$ for PlPc reflects the relatively low resolution of the diffraction data. The value of $\sigma_w(x)$ is reduced to 0.3 Å if the refinement restraints are treated as observations (Cruickshank, 1996).

3. Discussion

3.1. The structure of *P. laminosum* plastocyanin

The molecular structure of PlPc is shown in Fig. 1. The polypeptide fold is the same as found, with only minor variations, in all previous structure analyses of plastocyanin from plants, green algae and cyanobacteria (Table 4). The polypeptide forms a β-sandwich comprising seven β-strands and one irregular strand. The seven β-strands are arranged in two β-sheets (sheet 1: strands 2a, 1, 3, 6; sheet 2: strands 4, 7, 8, 2b). The only helical segment in the molecule begins with a turn of 3_{10} helix at the end of strand 4. It continues, after one non-helix residue, with two turns of α-helix at the beginning of the irregular strand 5, which is the region of greatest variability among plastocyanin structures. The Cu atom is located near one end of the molecule (the 'north' end) and is coordinated by the side chains of two His residues, a Cys and a Met. The coordination geometry is trigonal pyramidal with the Met ligand at the apex. The orientation of the copper site is such that the shortest pathway from the Cu atom to the molecular surface is *via* the imidazole ring of one of the His ligands (His92 in PlPc, corresponding to His87 in plant plastocyanins).

Figure 1
Molecular structure of *P. laminosum* plastocyanin, PlPc. Arrows represent β-strands. The polypeptide backbone is coloured according to sequence position between the N-terminus (blue) and the C-terminus (red). The Cu^{II} atom (blue) is coordinated by His39 (37), Cys89 (84), His92 (87) and Met97 (92). (The numbers cited in parentheses refer to the corresponding residue in plant plastocyanins, *e.g.* poplar plastocyanin.) Figure produced with *MOLSCRIPT* (Kraulis, 1991) and *RASTER3D* (Bacon & Anderson, 1988; Merritt & Murphy, 1994).

Table 4
Structure analyses of plastocyanin.

Type	Species	Method	References
Plants	Poplar	XRD	Colman *et al.* (1978); Guss & Freeman (1983); Guss *et al.* (1992)
	French bean	NMR	Moore *et al.* (1991)
	Parsley	NMR	Bagby *et al.* (1994)
Green algae	*Scenedesmus obliquus*	NMR	Moore *et al.* (1988)
	Enteromorpha prolifera	XRD	Collyer *et al.* (1990)
	Chlamydomonas reinhardtii	XRD	Redinbo *et al.* (1993)
Cyanobacteria	*Anabaena variabilis*	NMR	Badsberg *et al.* (1996)
		XRD	Fields *et al.* (1999)
	Synechocystis sp. PCC 6803	XRD	Romero *et al.* (1998)

As stated above (see §2.3), the asymmetric unit of PlPc comprises three molecules A, B and C, which are related by a non-crystallographic threefold axis (Fig. 2). Pairwise superpositions of the three molecules reveal no significant differences between the structures (Fig. 3, top three panels). The displacement parameters B are generally high ($\langle B \rangle$ = 34 Å^2). When plotted against the residue numbers in molecules A, B and C, the B values exhibit several common trends (Fig. 4). Low B values occur at residues 80–95 (the copper-binding loop between β-strands 7 and 8). High values occur in the regions of residues 20–25 (β-strand 2), residues 77–80 (the loop between β-strands 6 and 7) and residues 101–105 (the C-terminal end of β-strand 8).

3.2. The copper site

The Cu atom in PlPc is coordinated by His39 (37), Cys89 (84), His92 (87) and Met97 (92), where the numbers in parentheses indicate the corresponding residue labels in the usual bench-mark plastocyanin, poplar plastocyanin (PoPc). The coordination is roughly tetrahedral; on spectroscopic grounds it is best described as trigonal pyramidal, with Met97 S^{δ} in the apical position (Penfield *et al.*, 1981). The Cu–ligand distances for PlPc and PoPc are compared in Table 5.

Table 5
Cu–ligand distances (Å) in *P. laminosum* plastocyanin (PlPc, molecules A–C) compared with poplar plastocyanin (PoPc).

The Cruickshank (1996) 'diffraction data precision indicator' $\sigma_w(x)$ for the donor atoms in PlPc is 0.2 Å, after allowing for displacement-parameter effects ($\langle B \rangle$ = 22 Å^2 for ligand groups, 34 Å^2 overall) and after treating refinement restraints as observations. The Cu–ligand distances and e.s.d.s for PoPc are taken from a refinement at 1.33 Å resolution (Guss *et al.*, 1992). The ligand-residue numbers in PoPc are 37, 84, 87 and 92.

	Atom			
Molecule	His39 $N^{\delta1}$	Cys89 S^{γ}	His92 $N^{\delta1}$	Met97 S^{δ}
PlPc A	2.2	2.1	2.0	2.6
PlPc B	2.1	2.1	1.9	2.7
PlPc C	2.2	2.2	2.0	2.8
PoPc	1.91 (4)	2.07 (4)	2.06 (4)	2.82 (4)

Differences are not significant. The Cruickshank 'diffraction data precision indicator' $\sigma_w(x)$ for the donor atoms is 0.2 Å, after allowing for the below-average displacement parameters B (Table 3) and treating the refinement restraints as observations (Cruickshank, 1996). We regard this as a conservative estimate of the precision of the Cu–ligand distances.

3.3. The interstitial Zn^{2+} ions

Between each pair of the PlPc molecules related by the non-crystallographic threefold axis lies a Zn^{2+} ion (Fig. 2*a*). Since crystals could not be grown in the absence of Zn^{2+}, it is likely that the formation of trimers was a prerequisite for crystallization. Each Zn^{2+} ion is coordinated by His61 $N^{\varepsilon2}$ from one PlPc molecule and by Asp44 $O^{\delta2}$ and Asp45 $O^{\delta1}$ from another. These ligating atoms lie at three corners of a tetrahedron. For the Zn^{2+} ions between molecules A and B and molecules B and C, a solvent atom in the fourth coordination position was clearly identified in electron-density maps. Similar interstitial Zn^{2+} ions, coordinated by Asp/Glu and His side chains of two protein molecules, have been reported in the structure of another 'blue' Cu protein, *Pseudomonas putida* azurin (Chen *et al.*, 1998), as well as the structure of *Rhodobacter capsulatus*

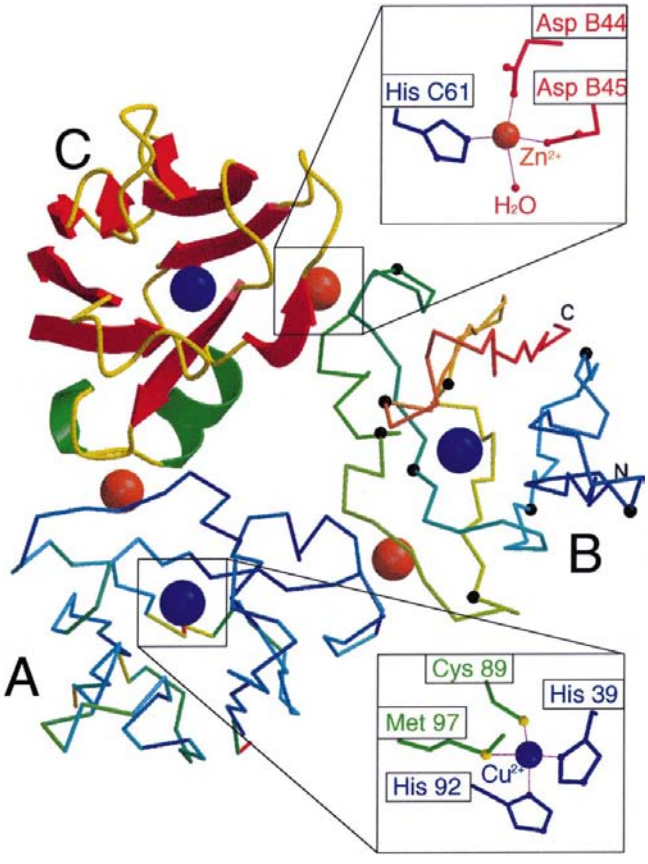

Figure 2
The three protein molecules in the asymmetric unit of PlPc viewed down the non-crystallographic threefold axis. The 'northern' end of each molecule is closest to the reader. Molecule A is represented by a Cα trace coloured according to the temperature factor of the main-chain atoms of each residue. Molecule B is represented by a Cα trace coloured as in Fig. 1. Every tenth Cα atom is marked with a black sphere. Molecule C is represented by a ribbon diagram showing strands as yellow arrows, helices as green ribbon and other secondary-structure elements as red coil. The upper inset shows the intermolecular Zn^{II} atom with its ligands. The lower inset shows the Cu^{II} atom with its ligands. Figure produced with the same software as Fig. 1.

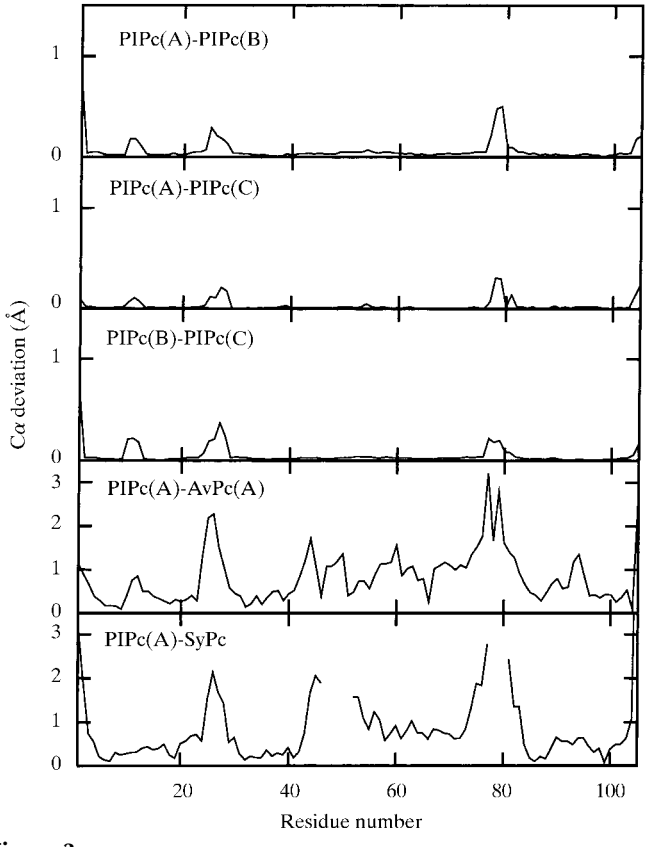

Figure 3
Upper three panels: differences between the positions of corresponding Cα atoms after pairwise superpositions of *P. laminosum* plastocyanin molecules A, B and C. Note that the vertical scale is different from that in the bottom section of the figure. Lower two panels: differences between the positions of corresponding Cα atoms after superposing *P. laminosum* plastocyanin (PlPc, molecule A) with *A. variabilis* plastocyanin (AvPc, molecule A) and with *Synechocystis* plastocyanin (SyPc, triple mutant, Protein Data Bank entry 1PCS). Gaps in the lower plot indicate residues in PlPc for which there is no equivalent residue in SyPc (see Fig. 5). Residues in a pair of superposed molecules were defined as 'equivalent' if their Cα atoms were separated by $\leq$3.8 Å. Figure produced using *LSQMAN* (Kleywegt & Jones, 1994*b*).

cytochrome c' (Tahirov *et al.* 1997). In the latter case, as in the present work, the Zn^{2+} ions were essential for crystallization.

3.4. Comparisons between PlPc and plant plastocyanins

P. laminosum plastocyanin has 105 amino-acid residues (Varley *et al.*, 1995), whereas the plastocyanins of higher plants and green algae have 97–99. In a structure-based alignment with a 99-residue plant plastocyanin (Fig. 5), two of the additional residues occur at the N-terminus, three at positions 78–80 and one at the C-terminus. The extensions at the N- and C-termini do not affect the polypeptide fold, and the additional residues at positions 78–80 merely add a hairpin bend to a loop at the the end of the molecule remote from the copper site (the 'south' end). However, there are two further differences between the structures of PlPc and plant plastocyanins: in PlPc, five residues at positions 51–55 replace a group of three residues in the plant plastocyanins, and one residue at position 62 replaces another group of three residues. These differences leave the total number of residues unchanged, but they are associated with a substantial structural rearrangement in the irregular fifth strand of the polypeptide. The two additional residues at 51–55 in PlPc are part of an additional turn of helix at residues 52–56, while the shortening of the polypeptide at residue 62 removes a bulge which occurs at residues 58–60 in plant plastocyanins.

From a functional point of view, the most important difference between PlPc and plant plastocyanins is that at neutral pH the PlPc molecule has a total charge of −3, compared with charges of −7 to −9 on plant plastocyanin molecules (including in each case +2 for the Cu atom and −1 for the copper-binding Cys). The difference between the charges is largely localized in the region of the 'acidic patch', which in plant plastocyanins occurs at residues 42–45 and 59–61. In PlPc the residues corresponding to the first of these two groups are Asp44–Asp45–Lys46–Gln47 and the residues corresponding to the second group are Ser62–Gln63 (Fig. 6). Thus, the two groups of acidic residues, which have attracted attention because they surround the invariant residue Tyr83 in plant plastocyanins, are missing in PlPc. Instead, the region around the invariant Tyr (Tyr88 in PlPc) has an overall basic character, to which Lys53 and Arg93 also contribute (Fig. 6). While the role of the invariant Tyr in physiological electron transfer is still uncertain, the presence of a basic region on the PlPc molecule is consistent with the observation that PlPc, when it reacts with the cytochrome b_6f complex, behaves as though it has a small net positive local charge (Wagner *et al.*, 1996).

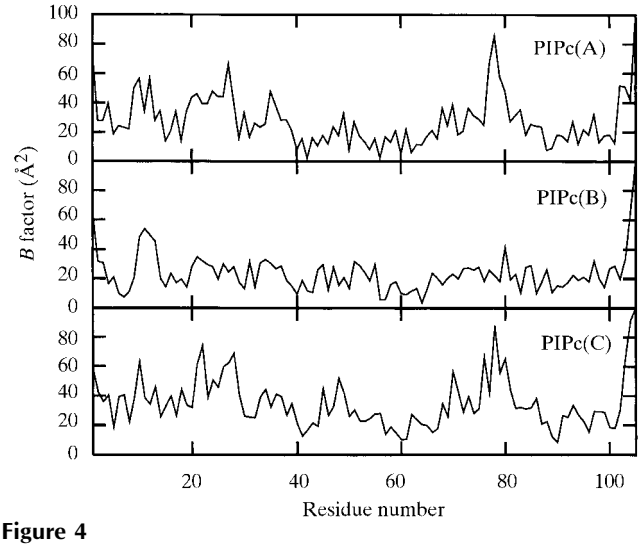

Figure 4
Temperature factors for the Cα atoms of the three independent molecules A, B and C of *P. laminosum* plastocyanin.

3.5. Comparisons between PlPc and other cyanobacterial plastocyanins

Two cyanobacterial plastocyanins have previously been characterized structurally: *A. variabilis* plastocyanin (AvPc) and *Synechocystis* plastocyanin (SyPc) (Table 4). A structure-based alignment of the sequences of PlPc, AvPc and SyPc is included in Fig. 5. The sequence of SyPc is seven residues shorter than the other two sequences, with two residues instead of five at positions 47–51, three residues missing between positions 78–82 and one residue missing at the C-terminus. A detailed analysis of the structural consequences of these sequence differences is in preparation (Fields *et al.*, 1999). Owing to the inclusion of additional structural information, the present alignment of SyPc with AvPc differs slightly from earlier proposals (Navarro *et al.*, 1997; Romero *et al.*, 1998).

Fig. 3 (bottom two panels) shows the differences between the positions of corresponding Cα atoms when PlPc is superposed in turn with AvPc and SyPc. The differences between corresponding Cα atomic positions are generally small, except

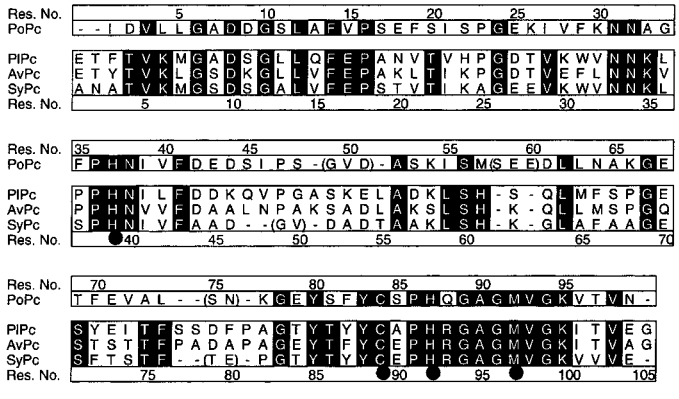

Figure 5
A structure-based sequence alignment of poplar plastocyanin (PoPc), *P. laminosum* plastocyanin (PlPc), *A. variabilis* plastocyanin (AvPc) and *Synechocystis* sp. PCC 6803 plastocyanin (SyPc). The residue numbers in the top row refer to PoPc and those in the bottom row refer to PlPc and AvPc. In each sequence, parentheses indicate residues that are not structurally equivalent to the residues listed vertically above or below them in the other sequences. The sequence shown for SyPc is that of the native protein (Briggs *et al.*, 1990); the coordinates used to align this sequence with the others were taken from the structure of a SyPc triple mutant (Protein Data Bank entry 1PCS). The sequences were aligned using *CLUSTALW* (Thompson *et al.*, 1994). Figure produced using *ALSCRIPT* (Barton, 1993).

at residues 23–26 (the β-turn between strands 2 and 3), 44–46 (a β-turn near the end of strand 4), 60 (end of helical segment in strand 5) and 79–81 (the β-hairpin bend between strands 6 and 7). A close similarity between the structures of PlPc and AvPc (r.m.s. difference = 1.1 Å) is to be expected in view of the high level of sequence identity (66%). The differences between PlPC and AvPc at residues 44–46 and 60 can be attributed to the presence of the Zn^{2+}-binding site at residues 44, 45 and 61 in PlPc. The large differences at residues 23–26 and 79–81 are associated with high displacement parameters in PlPc (Fig. 4), suggesting that these loops are disordered or flexible and hence determined with lower accuracy.

4. Conclusions

The structure of *P. laminosum* plastocyanin is closely similar to those of the plastocyanins from two other cyanobacteria, *Anabaena variabilis* and (with allowance for differences in the number of amino-acid residues) *Synechocystis* sp. PCC 6803 (A42D/D47P/A63L triple mutant). The absence of a concentration of negative surface charges corresponding to the acidic patch of plant plastocyanins is confirmed. The location and coordination of interstitial Zn^{2+} ions in PlPc crystals are consistent with the grouping of the protein molecules around a non-crystallographic threefold axis and explain why Zn^{2+} ions appear to be essential for crystallization.

This work was supported by grant A29601726 from the Australian Research Council to JMG and HCF. MJW thanks the Biotechnology and Biological Sciences Research Council (UK) for a Research Studentship.

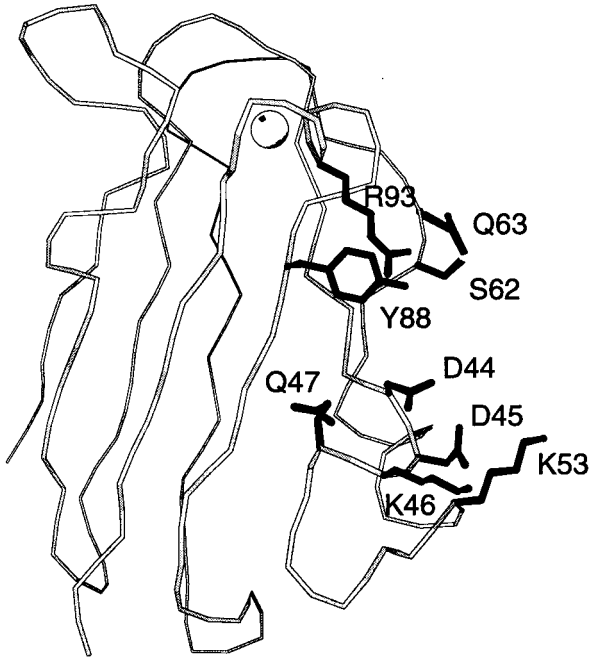

Figure 6
The surface residues near Tyr88 in *P. laminosum* plastocyanin are predominantly non-acidic. The sequences Asp44–Asp45–Lys46–Gln47 and Ser62–Gln63 correspond to the conserved negative patch formed by residues 42–45 and 59–61 in plant plastocyanins. The basic character of the surface near Tyr88 is enhanced by Lys53 and Arg93.

References

Bacon, D. J. & Anderson, W. F. (1988). *J. Mol. Graph.* **6**, 219–220.
Badsberg, U., Jorgensen, A. M., Gesmar, H., Led, J. J., Hammerstad, J. M., Jespersen, L. L. & Ulstrup, J. (1996). *Biochemistry*, **35**, 7021–7031.
Bagby, S., Driscoll, P. C., Harvey, T. S. & Hill, H. A. O. (1994). *Biochemistry*, **33**, 6611–6622.
Barton, G. J. (1993). *Protein Eng.* **6**, 37–40.
Bernstein, F. C., Koetzle, T. F., Williams, G. J. B., Meyer, E. F. Jr, Brice, M. D., Rodgers, J. P., Kennard, O., Shimanouchi, T. & Tasumi, M. (1977). *J. Mol. Biol.* **112**, 535–542.
Briggs, L. M., Pecoraro, V. L. & McIntosh, L. (1990). *Plant Mol. Biol.* **15**, 633–642.
Brünger, A. T. (1992). *X-PLOR*, *Version 3.1. A System for Crystallography and NMR.* Yale University Press, New Haven, CT, USA.
Chen, Z.-W., Barber, M. J., McIntire, W. S. & Mathews, F. S. (1998). *Acta Cryst.* D**54**, 253–268.
Collaborative Computational Project, Number 4 (1994). *Acta Cryst.* D**50**, 760–763.
Collyer, C. A., Guss, J. M., Sugimura, Y., Yoshizaki, H. & Freeman, H. C. (1990). *J. Mol. Biol.* **211**, 617–632.
Colman, P. M., Freeman, H. C., Guss, J. M., Murata, M., Norris, V. A., Ramshaw, J. A. M. & Venkatappa, M. P. (1978). *Nature (London)*, **272**, 319–324.
Cruickshank, D. W. J. (1996). *Proceedings of the CCP4 Study Weekend*, edited by E. Dodson, M. Moore, A. Ralph & S. Bailey, pp. 11–22. Warrington: Daresbury Laboratory.
Driessen, H. P. C. & Tickle, I. J. (1994). Unpublished work.
Engh, R. A. & Huber, R. (1991). *Acta Cryst.* A**47**, 392–400.
Fields, B. A., Freeman, H. C., Govinderaju, K., Guss, J. M., Jackman, M. P. & Sykes, A. G. (1999). In preparation.
Guss, J. M., Bartunik, H. D. & Freeman, H. C. (1992). *Acta Cryst.* B**48**, 790–811.
Guss, J. M. & Freeman, H. C. (1983). *J. Mol. Biol.* **169**, 521–563.
Hibino, T., Lee, B. H., Yajima, T., Odani, A., Yamauchi, O. & Takabe, T. (1996). *J. Biochem. (Tokyo)*, **120**, 556–563.
Hippler, M., Reichert, J., Sutter, M., Zak, E., Altschmied, L., Schoer, U., Hermann, R. G. & Haehnel, W. (1996). *EMBO J.* **15**, 6374–6384.
Jones, T. A., Zou, J.-Y., Cowan, S. W. & Kjeldgaard, M. (1991). *Acta Cryst.* A**47**, 110–119.
Kannt, A., Young, S. & Bendall, D. S. (1996). *Biochim. Biophys. Acta*, **1277**, 115–126.
Kleywegt, G. J. & Jones, T. A. (1994*a*). *Proceedings of the CCP4 Study Weekend*, pp. 59–66. Warrington: Daresbury Laboratory.
Kleywegt, G. J. & Jones, T. A. (1994*b*). *ESF/CCP4 Newslett.* **31**, 9–14.
Kleywegt, G. J. & Jones, T. A. (1996). *Structure*, **4**, 1395–1400.
Kraulis, P. J. (1991). *J. Appl. Cryst.* **24**, 946–950.
Lee, B. H., Hibino, T., Takabe, T. & Weisbeek, P. J. (1995). *J. Biochem. (Tokyo)*, **117**, 1209–1217.
Matthews, B. W. (1977). *The Proteins*, edited by H. Neurath & R. L. Hill, Vol. III, pp. 468–477. New York: Academic Press.
Merritt, E. A. & Murphy, M. E. P. (1994). *Acta Cryst.* D**50**, 869–873.
Moore, J. M., Case, D. A., Chazin, W. J., Pippert, G. P., Havel, T. F., Powls, R. & Wright, P. E. (1988). *Science*, **240**, 314–317.
Moore, J. M., Lepre, C. A., Gippert, G. P., Chazin, W. J., Case, D. A. & Wright, P. E. (1991). *J. Mol. Biol.* **221**, 533–555.
Navarro, J. N., Hervás, M. & de la Rosa, M. A. (1997). *J. Biol. Inorg. Chem.* **2**, 11–22.
Navaza, J. (1994). *Acta Cryst.* A**50**, 157–163.

Otwinowski, Z. (1993). *Proceedings of the CCP4 Study Weekend*, pp. 56–62. Warrington: Daresbury Laboratory.
Penfield, K. W., Gay, R. R., Himmelwright, R. S., Eickman, N. C., Norris, V. A., Freeman, H. C. & Solomon, E. I. (1981). *J. Am. Chem. Soc.* **103**, 4382–4388.
Redinbo, M. R., Cascio, D., Choukir, M. K., Rice, D., Merchant, S. & Yeates, T. O. (1993). *Biochemistry*, **32**, 10560–10567.
Redinbo, M. R., Yeates, T. O. & Merchant, S. (1994). *J. Bioenerg. Biomembr.* **26**, 49–66.
Romero, A., de la Cerda, B., Varela, P. F., Navarro, J. A., Hervás, M. & de la Rosa, M. A. (1998). *J. Mol. Biol.* **275**, 327–336.
Tahirov, T. H., Misaki, S., Meyer, T. E., Cusanovich, M. A., Higuchi, Y. & Yasuoka, H. (1997). *Acta Cryst.* D**53**, 658–664.
Thompson, J. D., Higgins, D. G. & Gibson, T. J. (1994). *Nucleic Acids Res.* **22**, 4673–4680.
Ubbink, M., Ejdebaeck, M., Karlsson, B. G. & Bendall, D. S. (1998). *Structure*, **6**, 323–335.
Varley, J. P. A., Moehrle, J. J., Manasse, R. S., Bendall, D. S. & Howe, C. J. (1995). *Plant Mol. Biol.* **27**, 179–190.
Wagner, M. J., Packer, J. C. L., Howe, C. J. & Bendall, D. S. (1996). *Biochim. Biophys. Acta*, **1276**, 246–252.